Ab Initio Calculations of Carbonyl Adsorption Complexes at Zeolitic Brönsted Sites Simulated by Model Clusters: Role of Modeling

E. Kassab,*,† H. Jessri,† M. Allavena,*,† and D. White‡

Laboratoire de Chimie Théorique, CNRS−UMR 7616, Université P. et M. Curie, Tour 22-23, Case 137, 4 place Jussieu, 75252 Paris Cedex 05, France, and Department of Chemistry, University of Pennsylvania, Philadelphia, PA 19104

Received: July 16, 1998; In Final Form: January 14, 1999

Three different model clusters simulating the acid site in zeolites are employed to explore the stability of the hydrogen bonded adsorption complex and silyl−ether addition compounds on adsorption of the carbonyls formaldehyde, acetaldehyde, and acetone at the Brönsted acid site. Ab initio calculations are performed at the Hartree−Fock level and post-Hartree−Fock. Optimization along a reaction coordinate in the case of these carbonyls exhibits a competition between two stable structures, hydrogen bonded and addition complexes. The relative stabilities of these two complexes are shown to be very much dependent on the nature of the cluster model. Effects of basis set superposition error and correlation are also discussed.

I. Introduction

The simulation of catalytic reactions by acidic zeolites has raised many questions concerning the nature of molecule−zeolite complexes that prepare the adsorbed molecule for nucleophilic attack. In the case of weak bases, the initial step in the acid−base chemistry invariably involves the formation of a hydrogen bonded complex between the acidic bridging hydroxyl in the zeolite and the adsorbed weak base. The key step in the acidic catalysis is then the activation of the complex by proton transfer. In the case of the alkylation reactions involving adsorbed alcohols[1] or alkenes,[2] the subsequent proton transfer from the zeolite to the adsorbat leads to a silyl ether which has been experimentally observed.[3] However, in the case of condensation reactions involving ketones or aldehydes, proton transfer may induce the formation of a silyl−ether addition compound as shown schematically below.

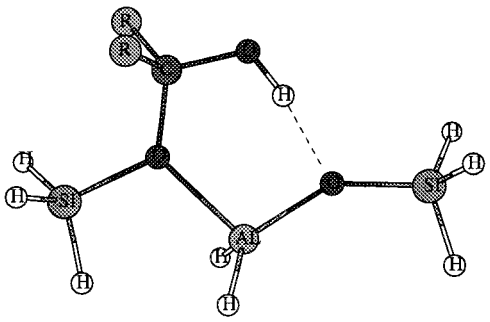

This analogue of the enol form of the H-bonded adsorption complex, has neither been experimentally identified nor except for adsorbed acetone[4] theoretically explored, even though the enol form has been postulated as the reactive species in the aldol condensation reactions. In the case of acetone, the calculations have been extended to a level which includes full optimization.

In this paper, we examine the structure and stability of such adsorption complexes for a series of adsorbed carbonyls, where R an R′ can be either H atoms or methyl groups. This is an extension of our earlier studies of the acetone complex (ref 4) where we use a cluster model to simulate the zeolite. The choice of the cluster model used here is dictated by the limitations imposed by the available computational facilities for a calculation that takes into account full optimization and electron correlation corrections. Use of periodic methods is ruled out in the present calculation for two main reasons: (i) the absence of correlation corrections in periodic methods, a prerequisite for proper treatment of reactivity, and (ii) the requirement of translational symmetry which imposes to use a unit cell larger than the crystallographic one, to reduce the interaction between the adsorbats artificially introduced. Admittedly the use of a cluster model neglects the effects of "embedding" which have already been discussed in detail.[5] However, since the most important interaction affecting the reaction pathway is highly localized, the cluster model approach should provide some insight as to the importance of the silyl−ether complex in the mechanism of the reaction catalyzed by solid acids.

The manuscript is divided into five parts. Part II describes the methodology and models used in the calculation. Part III presents the results of the calculation for the isolated carbonyl-containing molecules and clusters. In part IV, the results relating to the formation of molecule−cluster complexes are given as well for several intermediates along the reaction pathway. Finally, part V is a discussion of results.

II. Methodology

As in our earlier calculations of the acetone−zeolite complex, the all-electron Hartree−Fock method is adopted with a 6-31G* basis set functions. To verify that a basis sets extension beyond 6-31G* would not seriously affect our results, two calculations have been performed with basis sets 6-31+G* and 6-31++G** for some specific cases indicated further in the text. Correction for electronic correlation is calculated by using Moller−Plesset perturbation theory to second order (MP2). Three series of calculations have been performed, one using geometry deter-

* Corresponding authors.
† Université P. et M. Curie.
‡ University of Pennsylvania.

10.1021/jp983048w CCC: $18.00
Published on Web 03/26/1999

TABLE 1: Calculated Energies and Electronic Properties of Isolated Molecules Using 6-31G* Basis Set (Total Electronic Energies (*E*), Zero-Point Energy Corrections (ZPE), Proton Affinities (PA), Bond Length of CO Bond (*r*), Dipole Moment (μ), and Harmonic Stretching Frequencies (ω_{CO}))

		H_2CO	CH_3HCO	$(CH_3)_2CO$
HF	*E* (au)	−113.86633	−152.91597	−191.96224
				(−191.96760)[e]
				(−191.97740)[f]
	ZPE (au)	0.02920	0.05993	0.08991
	PA (kcal/mol)	182.0	194.2	203.7
	r (Å)	1.184	1.188	1.192
	μ (D)	2.666	2.982	3.119
				(3.363)[e]
				(3.372)[f]
	ω_{CO} (cm^{-1})	2028.1	2031.8	2022.1
MP2//MP2	*E* (au)	−114.16775	−153.34692	−192.52390
	ZPE (au)	0.02729	0.05696	0.08593
	PA (kcal/mol)	180.8	186.5	196.1
		(171.7)[a]	(186.6)[a]	(196.7)[a]
	r (Å)	1.221	1.223	1.228
		(1.210)[b]	(1.216)[b]	(1.215)[b]
	μ (D)	2.778	2.619	2.774
		(2.33)[c]	(2.69)[c]	(2.89)[c]
	ω_{CO} (cm^{-1})	1788	1797.2	1791.7
		(1746)[b]	(1743)[b]	(1731)[d]

[a] *J. Phys. Chem. Ref. Data*. **1984**, *13*, 707. [b] Herzberg, H. Molecular Spectra and Molecular Structure; Vol. III. D. van Nostrand Reinhold: New York, 1972. [c] Handbook of Chemistry and Physics 62nd ed.; CRC Press, Inc.: Boca Raton, 1981−82. [d] Shimanouchi, T. Tables of Molecular Vibrational Frequencies, Consolidated Volume I; National Bureau of Standards NSRDS−NBS 39, 1972. [e] Calculated at HF/6-31+G*//6-31+G* level. [f] Calculated at HF/6-31++G**//6-31+G* level. [g] Experimental data are indicated in parenthesis.

mined at the Hartree−Fock level (MP2//HF) and an other one where both energy and geometry are optimized at the MP2 level (MP2//MP2). In the tables, only results corresponding to HF and MP2//MP2 approximations are given. Intermediate results (MP2//HF) may be obtained by request to the authors. All calculations are performed with the GAUSSIAN-94 program.[6]

For optimizations, a two-step procedure is adopted. Calculations are first initiated with a geometrical configuration corresponding to hydrogen bonded complexes ZOH···B where ZOH and B designate the proton donor and acceptor, respectively. The *r*(O−H) distance is fixed, and the rest of the system is relaxed. Next the *r*(O−H) distance is changed to explore a section of the potential energy surface (PES) in order to determine the extremal regions. At the various energy minima a full optimization is performed again in order to obtain more accurate values of the geometrical parameters, including the *r*(O−H) distance of the most stable conformation. In regions of higher energy, secondary minima or transition states, the following strategy is adopted. The Hessian matrix is calculated, and in the event a negative eigenvalue is detected (saddle point), a series of optimizations for different values of *r*(O−H) are again performed starting from the saddle point, to verify that the transition state is one connecting the absolute minima with the secondary minima obtained during the initial optimization.

For calculations of the components of the shielding chemical tensor, the GIAO method[7] has been used in conjunction with the TEXAS-90 program.[8]

III. Isolated Clusters and Adsorbate Molecules

To test the accuracy of methodology, calculations of the energetics and electronic properties of the isolated carbonyl molecules were performed and the results compared with experiment.

For the isolated carbonyl H_2CO, CH_3HCO, and $(CH_3)_2CO$, the following properties have been calculated and compared with experimental data where available: total electronic energies (*E*) and zero-point vibrational energy correction (ZPE), which will be necessary for estimating dissociation energies of the ZOH··· B complex, proton affinity (PA), the C−O internuclear distance (*r*), the harmonic frequency (ω_{CO}) of the CO stretching mode, and the molecular dipole moment (μ). In Table 1, the results at the HF and MP2//MP2 levels are given. In going from HF to the MP2//MP2 level, the main effect is in the values of ω and μ which are now in better agreement with experiment. With increasing molecular weight, the experimental trends in the other properties are rather well reproduced even at the HF level.

TABLE 2: ^{13}C Chemical Shift of Isolated Species (in ppm)

	$H_2^{13}CO$		$(CH_3)H^{13}CO$		$(CH_3)_2^{13}CO$	
	a	*b*	*a*	*c*	*a*	*d*
σ^r_{xx}	274.0	274.2	281.2	285.0 ± 2.5	279.0	283.0 ± 2
σ^r_{yy}	190.7	212.5	199.0	231.0 ± 2.5	226.0	272.0 ± 2
σ^r_{zz}	71.9	85.0	73.2	84.0 ± 2.5	72.0	84.0 ± 2
σ^r_{iso}	178.9	190.6	184.9	200.0 ± 2.5	192.0	213.0 ± 1
						(202.0 ± 1)[e]

[a] This work, TEXAS 90/HF/6-31G*. [b] Reference 9. [c] Reference 10. [d] Solide acetone (78 K). [e] Gaseous acetone (300 K), see ref 4. [f] Theoretical results are given with respect to calculated TMS: $\sigma^r = 201.8 - \sigma^{abs}$ where σ^r is the relative value given in the table and σ^{abs} the calculated absolute value. $\sigma^r_{iso} = (1/3)(\sigma_{xx} + \sigma_{yy} + \sigma_{zz})$.

The calculated ^{13}C components along the principal axes of the chemical shielding tensor for the various carbonyls are given in Table 2. The component σ_{yy} lies in the direction of the σ-bond of CO double bond, σ_{xx} perpendicular to σ_{yy} in the sp^2 plane, and σ_{zz} perpendicular to that plane. In the case of formaldehyde one can make a comparison between theory and experiment since the latter values were calculated from measured spin−rotation constants.[9] In the cases of acetaldehyde and acetone, the experimental data are for matrix-isolated species and the solid (ref 4), respectively. Here σ_{33}, the most shielded measured component, is identified with σ_{zz} and σ_{11}, the least shielded, with σ_{xx}. However, one can estimate the corrections to the gas phase by scaling the measured components by the difference between solid and gas-phase isotropic shifts given in parentheses. In general, there appears to be fair agreement between theory and experiment for the least and most shielded component

TABLE 3: Calculated Energies and Electronic Properties of Isolated Clusters Using 6-31G* Basis Set (Total Electronic Energies (E) and Zero-Point Energy Corrections (ZPE))[e]

	parameter	unit	ZOH(1)	ZOH(2)	ZOH(F)	ZOH(RS)	ZOH(RS,F)
HF	*E*	(au)	−394.58747	−974.83625	−974.79614	−4101.65924	−4101.55513
				−974.84604[c]			
				−974.86335[d]			
	ZPE	(au)	0.05628	0.09038	0.09132		
	r(OH)	(Å)	0.956	0.954	0.963	0.954	0.962
	r(AlO(H))	(Å)	2.026	2.001	1.746[b]	1.875	1.746[b]
	∠AlO(H)Si	(deg)	115.7[a]	135.5	142.6[b]	125.8	142.6[b]
	∠OAlO(H)	(deg)	88.2	90.9	110.6[b]	93.8	110.6[b]
	ω(OH)	(cm^{-1})	3991.6	4045.0	3896.2		
MP2//MP2	*E*	(au)	−395.01480	−975.40973	−975.36837		
	ZPE	(au)	0.05358	0.08713	0.08769		
	r(OH)	(Å)	0.985	0.979	0.963		
	r(AlO(H))	(Å)	2.035	2.003	1.746[b]		
	∠AlO(H)Si	(deg)	113.2[a]	138.5	146.6[b]		
	∠OAlO(H)	(deg)	84.6	86.9	109.3[b]		
	ω(OH)	(cm^{-1})	3602.7	3709.8	3609.0		
	Δ*E*	(au)	−0.42733	−0.57155	−0.57223		
	ΔZPE	(au)	0.00270	0.00862	0.00363		
	Δ*r*(OH)	(Å)	0.029	0.025	0.0		
	Δ*r*(AlO(H))	(Å)	0.009	0.001	0.0		
	Δ(∠AlO(H)Si	(deg)	−2.6	3.1	0.0		
	Δ(∠OAlO(H)	(deg)	−3.6	−4.0	0.0		
	Δω(OH)	(cm^{-1})	−388.9	−335.2	−287.2		

[a] In the ZOH(1) cluster, this angle corresponds to ∠AlOH. [b] Reference 12. [c] Calculated at HF/6-31+G*//6-31G*. [d] Calculated at HF/6-31++G**//6-31G*. [e] Geometrical parameters correspond to Figure 1. Magnitude of correlation effects $\Delta q = q(\text{MP2}) - q(\text{HF})$, for $q = E$, ZPE, and geometrical parameters, are shown in bottom row.

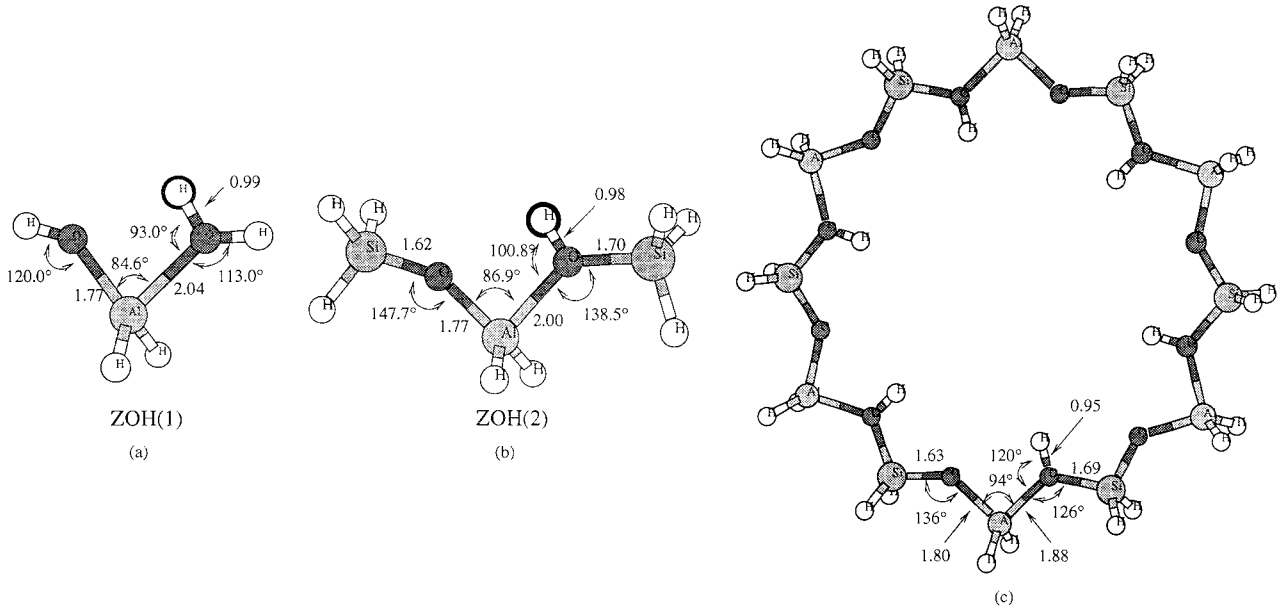

Figure 1. (a), (b) Structure of ZOH(1) and ZOH(2) isolated clusters resulting from full optimization at the MP2//MP2 level. Distances in angstroms and angles in degrees. (c) Structure of the ZOH(RS) cluster resulting from optimization at the HF level under summetry constraints.

but poor agreement for the component along the C═O direction. This is the component which is most sensitive to changes of the molecular electron density.[11]

In the present calculations, three different cluster models have been used. The $HOHAlH_2OH$ and $H_3SiOHAlH_2OSiH_3$ systems, respectively, designated as ZOH(1) and ZOH(2), have been fully optimized at the HF and MP2//MP2 level. The stoichiometry of the third cluster ZOH(F) is identical to ZOH(2), but the geometrical parameters are fixed. These parameters have been extracted from the experimental data of Mortier et al.[12] for Faujasite. The main interest of this ZOH(F) model is to investigate the role of framework relaxation in the formation of the B/ZOH complex. A larger cluster has also been used in order to estimate size effects on calculated quantities. This cluster is a ring structure constructed from 12 tetrahedral units and is designated as ZOH(RS). Calculations with this cluster are restricted to HF level with a 6-31G(5d) basis set functions instead of the 6-31G(6d) basis set used for all the other clusters. This has a small effect on the calculated energies but saves considerable computer time. Furthermore, calculations for the ZOH(RS) cluster are performed under the symmetry constraints of a planar ring structure with a C_6 symmetry axis and fixed terminal hydrogen atoms. The optimized geometrical parameters and ω(O−H) are given in Table 3. A schematic representation of the ZOH(*i*) clusters is given in Figure 1. The calculated Al−O bond length is longer than that of Si−O. This is reasonable considering the differences in ionic radii; however, this has not been verified experimentally since the crystallographic data[13]

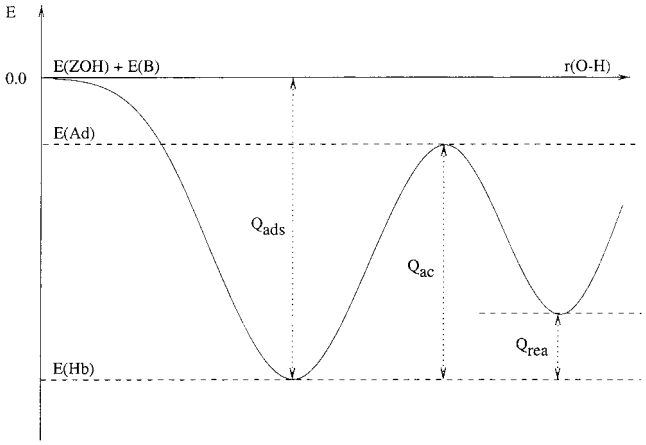

Figure 2. Schematic representation of the potential energy surface (PES) with definition of characteristic quantities Q_{ad}, Q_{ac}, Q_{rea}.

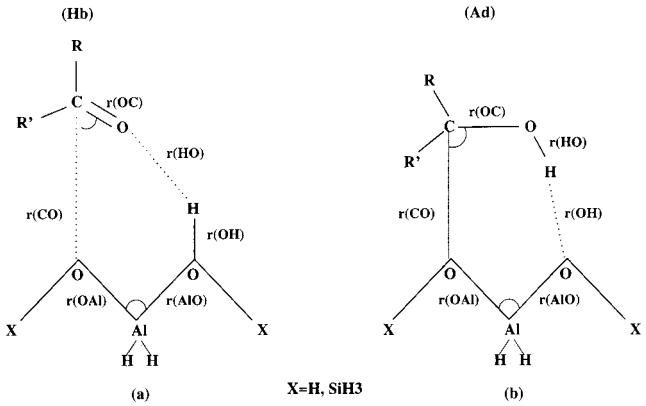

Figure 3. Hydrogen bonded (Hb) and addition (Ad) complex structures.

does not distinguish between the two substituents. In protonated zeolites, the average OTO angle is approximately 110° [14] which is 20° larger than for the optimized cluster structures. This is probably a consequence of the absence of ring closure in the cluster.

The calculated frequencies of the isolated clusters, ω(O−H) at the MP2//MP2 level (Table 3) fall in the range observed experimentally for HZSM-5 (3600 cm^{-1}) and the supercage of faujasite (3640 cm^{-1})[15,16] in which the OH group is less coupled to the framework than in the sodalite cage. In-plane δ (OH) and out-of-plane γ (OH) modes can be found in the set of frequencies resulting from ab initio calculation of vibrational properties. For ZOH(F), within the (MP2//MP2) approximation, a tentative attribution leads to 1290.4 and 290.4 cm^{-1}, respectively, which should be compared with the measurements of Jacobs et al.[17,18] at 1089 and 419 cm^{-1} respectively.

IV. Adsorption Complexes

a. Energetics and Structure. For each type of adsorption complex (Hb or Ad), nine base−clusters pairs can be formed, they are designated in what follows by B(n)/ZOH(i) where B(n) = $H_{2-n}(CH_3)_nCO$ with n = 0, 1, 2, and index i = 1,2, F designates the three clusters. In Figure 2, a typical profile of a section of the (PES) along the reaction coordinate r(O−H) for one of these base−cluster systems has been displayed. In general, two stable states are expected. The minimum at short r(O−H) distances (∼1 Å) corresponds to the hydrogen-bonded (Hb) complex shown in Figure 3a. The second minimum at longer r(O−H) distance corresponds to the silyl−ether addition compound (Ad) in which a C−O bond is formed (Figure 3b). The two minima are most often related by a transition state (TS) as depicted in Figure 2. When discussing energetics, reference will be made to three fundamental quantities defined as follows:

the heat of adsorption,

$$Q_{ad} = E(\mathrm{Hb}) - [E(\mathrm{ZOH}) + E(\mathrm{B})] \quad (1)$$

the heat of reaction,

$$Q_{rea} = E(\mathrm{Ad}) - E(\mathrm{Hb}) \quad (2)$$

and the activation energy,

$$Q_{ac} = E(\mathrm{TS}) - E(\mathrm{Hb}) \quad (3)$$

For accuracy, these quantities must be corrected for the zero-point energy defect (ZPE) and basis set superposition error (BSSE). The BSSE is calculated by using the counterpoise method and taking into account the effect of geometrical reconstruction:

$$\Delta E(\mathrm{BSSE}) = [E(\mathrm{ZOH})_{\phi(\mathrm{B/ZOH})} - E(\mathrm{ZOH})_{\phi(\mathrm{ZOH})} + E(\mathrm{B})_{\phi(\mathrm{B/ZOH})} - E(\mathrm{B})_{\phi(\mathrm{B})}] \quad (4)$$

where the differences in energies on the right-hand side have been calculated for two sets of wave functions ϕ(j), one corresponding to the complex, ϕ(B/ZOH), and the other to one of the components making up the complex, i.e., the cluster, ϕ-(ZOH), and the base, ϕ(B). It is evident from the definition of BSSE that such a correction is not required for Q_{rea} or Q_{ac}.

The calculations lead to two distinct minima, the (Ad) state becoming less and less stable when n or i are increasing. However, when using the ZOH(F) cluster model, the (Ad) does not form for n = 1 or 2.

The difference in energy between the optimized and frozen cluster

$$E(\text{optimized system}) - E(\text{frozen system}) = E_{relax} \quad (5)$$

where system refers to either an isolated cluster or a complex, defines a relaxation energy, E_{relax}, for the system when the structure is optimized. For the ZOH(2) cluster, E_{relax} amounts to −25.1 kcal/mol, and for the hydrogen bonded complex (Hb), E_{relax} equals −21.1, −20.9, and −18.4 kcal/mol for the complexed H_2CO, CH_3HCO, and $(CH_3)_2CO$, respectively, at the HF level and somewhat smaller at the MP2//MP2 level. For the silyl−ether addition complex with formaldehyde, E_{relax} = −26.9 kcal/mol at the HF level and −27.6 kcal/mol at MP2//MP2. When the ZOH(RS) cluster is used to form the complex, E_{relax} = −65.4 kcal/mol (isolated cluster) and −63.3 kcal/mol when complexed to H_2CO. However, this relaxation energy cannot be directly compared with the relaxation of the smaller cluster ZOH(2), both isolated and complexed, because the two clusters ZOH(2) and ZOH(RS) do not have the same stoichiometry. Assuming an equipartition of relaxation energy among the Al−O bonds (the bonds most affected by relaxation) it is possible to define a relaxation energy per Al−O bond by dividing each calculated E_{relax} by the number of Al−O bonds in each system, namely, 2 for ZOH(2) and 12 for ZOH(RS). For the isolated cluster, one obtains (in kcal/mol) −12.6 (ZOH-(2)) versus −5.5 (ZOH(RS)), when complexed with H_2CO, −10.6 (ZOH(2)/H_2CO) versus −5.3 (ZOH(RS)/H_2CO). The trends on complexing are similar for the two cases, but the amount of relaxed energy is smaller for ZOH(RS) cluster, in

TABLE 4: Calculated Total Electronic Energies (*E*) and Zero-Point Energy Corrections (ZPE) of (Hb), (TS), and (Ad) Complexes B(*n*)/ZOH(i) Using 6-31G* Basis Set (in au)

systems		HF		MP2//MP2	
		E	ZPE	*E*	ZPE
(Hb)	ZOH(1)	−508.47364	0.08863	−509.20568	0.08419
	ZOH(2)	−1088.72165	0.12291	−1089.60280	0.11775
H_2CO	ZOH(F)	−1088.68797	0.12367	−1089.56768	0.11810
	ZOH(RS)	−4215.54328			
	ZOH(RS,F)	−4215.44246			
	ZOH(1)	−547.52270	0.11878	−548.38426	0.11325
CH_3HCO	ZOH(2)	−1127.77160	0.15292	−1128.78321	0.14573[a]
	ZOH(F)	−1127.73831	0.15357	−1128.74863	0.14636[a]
	ZOH(1)	−586.56974	0.14848	−587.56304	0.14209
$(CH_3)_2CO$	ZOH(2)	−1166.81965	0.18285	−1167.95690[b]	0.17426[a]
		(−1166.83313)[c]			
		(−1166.85992)[d]			
	ZOH(F)	−1166.78686	0.18323	−1167.92545[b]	0.17462
(TS)	ZOH(1)	−508.44904	0.08793	−509.19487	0.08447
H_2CO	ZOH(2)	−1088.69134	0.12164	−1089.58634	0.11623
	ZOH(1)	−547.49750	0.11629	−548.37343	0.11237
CH_3HCO	ZOH(2)	−1127.74498	0.15519	*e*	
	ZOH(1)	−586.54144	0.14682	−587.54817	0.14036
$(CH_3)_2CO$	ZOH(2)	*e*		*e*	
(Ad)	ZOH(1)	−508.48552	0.09494	−509.21801	0.08974
H_2CO	ZOH(2)	−1088.72751	0.12925	−1089.61260	0.12342
	ZOH(F)	−1088.68469	0.12921	−1089.56864	0.12284
	ZOH(1)	−547.52672	0.12444	−548.39230	0.11832
CH_3HCO	ZOH(2)	−1127.76644	0.15891	−1128.78604	0.15144
	ZOH(F)	*f*		*f*	
$(CH_3)_2CO$	ZOH(1)	−586.56835	0.15355	−587.56867	0.14642
	ZOH(2)	−1166.80103	0.18804	−1167.95198[b]	
		(−1166.81283)[c]			
		(−1166.83964)[d]			

[a] When harmonic frequencies are not calculated, the ZPE is obtained from the ZPE calculated at HF level multiplied by 0.953. The scaling factor is deduced from comparison of HF and MP2 calculations performed on smaller systems. [b] Not optimized at MP2 level. [c] Calculated at HF/6-31+G*//6-31G* level. [d] Calculated at HF/6-31++G**//6-31G* level. [e] Not calculated. [f] Optimization failed to find a local minimum.

part, because of the symmetry constraints imposed on the larger cluster, which prevent full relaxation.

Calculation of the (TS) energy levels requires a computational effort which exceeds the one required for stationary states. On this account and because some (Ad) states are unstable only five (TS) states have been determined. They are the states associated to the B(*n*)/ZOH(*i*) complexes for $n = 0, 1$, $i = 1, 2$ and for $n = 2$, $i = 1$. In each case, the calculations have been performed at the HF and MP2//MP2 levels. As can be verified by inspection of the results, the nature of the (TS) is rather dependent on cluster model and methodologies. In most cases, the (TS) have a zwitterionic character. However, introduction of correlation effects diminishes the ionic character to the advantage of more neutral (concerted) structures where proton migration and formation of a CO bond (between the C of carbonyls and the basic oxygen of ZOH(*i*)) occur simultaneously. In the case of $n = 0$, $i = 1$, the (TS) remains neutral at any level of calculations. Finally, it should be pointed out that the activation energies for carbonyl addition complexes, when occurring, are systematically lower than those calculated within similar models for alkyl addition complexes. This could be expected on account of their gas-phase proton affinities, 717.7 ($n = 0$) and 822.2 ($n = 1$) kJ/mol, compared to 681.3 (ethylene) and 752.4 (propene) kJ/mol (ref 2).

Numerical results are reported in the following tables which contain all data deduced from optimization of the total energy of the three types of complexes (Hb), (TS), and (Ad). Energy levels of equilibrium conformations are presented in Table 4,

TABLE 5: Geometrical Parameters, as Defined in Figure 3, Distances in Å and Angles in Degrees[a]

systems		geometrical parameters					
		∠OAlO	*r*(O−H)	*r*(H−O)	*r*(O−C)	*r*(C−O)	∠OCO
(Hb)	ZOH(1)	96.5	0.969	1.801	1.196	3.164	92.4
		(96.8)	(0.999)	(1.743)	(1.234)	(3.078)	(96.0)
	ZOH(2)	99.8	0.969	1.786	1.195	3.396	91.0
		(99.6)	(1.002)	(1.700)	(1.234)	(3.217)	(98.8)
H_2CO	ZOH(F)	109.3	0.988	1.716	1.197	3.234	83.7
		(109.3)	(1.030)	(1.621)	(1.235)	(3.117)	(88.4)
	ZOH(RS)	94.0	0.971	1.840	1.193	3.619	68.5
	ZOH(RS,F)	110.6	0.983	1.807	1.195	3.573	64.3
	ZOH(1)	97.3	0.969	1.794	1.199	2.885	95.4
		(98.0)	(1.000)	(1.711)	(1.233)	(2.738)	(97.0)
CH_3CHO	ZOH(2)	97.5	0.969	1.774	1.197	3.794	71.5
		(99.6)	(1.002)	(1.700)	(1.234)	(3.217)	(98.8)
	ZOH(F)	109.3	0.986	1.720	1.200	3.793	65.5
		(109.3)	(1.034)	(1.577)	(1.238)	(3.142)	(73.3)
	ZOH(1)	97.4	0.968	1.789	1.204	3.010	90.6
		(98.2)	(1.002)	(1.687)	(1.237)	(2.824)	(91.4)
$(CH_3)_2CO$	ZOH(2)	101.7	0.972	1.751	1.203	4.428	70.1
	ZOH(F)	109.3	0.994	1.656	1.207	3.535	70.5
(TS)	ZOH(1)	94.6	1.113	1.292	1.257	1.782	107.9
		(96.9)	(1.107)	(1.361)	(1.272)	(1.838)	(108.4)
H_2CO	ZOH(2)	99.0	1.327	1.091	1.233	2.155	100.3
		(96.6)	(1.181)	(1.251)	(1.268)	(1.936)	(105.5)
	ZOH(1)	96.2	1.276	1.119	1.246	2.060	102.6
		(96.9)	(1.141)	(1.303)	(1.276)	(1.879)	(106.5)
CH_3CHO	ZOH(2)	99.7	1.588	0.999	1.255	2.120	99.4
$(CH_3)_2CO$	ZOH(1)	96.9	1.388	1.057	1.252	2.203	97.6
		(97.1)	(1.177)	(1.253)	(1.283)	(1.917)	(104.6)
(Ad)	ZOH(1)	94.0	1.926	0.960	1.353	1.445	110.9
		(95.0)	(1.773)	(0.995)	(1.368)	(1.483)	(110.0)
H_2CO	ZOH(2)	96.5	2.130	0.955	1.358	1.445	110.4
		(95.2)	(1.883)	(0.988)	(1.375)	(1.481)	(110.0)
	ZOH(F)	109.3	2.139	0.957	1.342	1.544	109.3
		(109.3)	(1.950)	(0.993)	(1.349)	(1.611)	(109.3)
CH_3CHO	ZOH(1)	95.0	1.924	0.961	1.360	1.457	109.5
		(96.0)	(1.786)	(0.995)	(1.376)	(1.494)	(109.7)
	ZOH(2)	98.2	2.077	0.955	1.363	1.462	108.8
		(96.4)	(1.891)	(0.989)	(1.382)	(1.497)	(108.5)
$(CH_3)_2CO$	ZOH(1)	95.7	1.867	0.961	1.375	1.460	109.4
		(96.4)	(1.775)	(0.996)	(1.381)	(1.505)	(108.5)
	ZOH(2)	101.2	1.872	0.957	1.359	1.495	107.4

[a] Optimization at HF level using 6-31G*. Results from optimization at MP2//MP2 level are given in parenthesis.

and corresponding structural parameters are given in Table 5. In Table 6, the differences in energy corresponding to the various *Q*'s defined above (formulas 1−3) are summarized. In the case of acetone, our former results (ref 4) have been improved by relaxing the relative orientation of the two terminal CH_3 groups, which were previously kept fixed in an eclipsed configuration. Both the uncorrected and corrected heats for ZPE and BSSE are given. It should be noted that the corrections amount to as much as 30% in many cases.

Relative positions of energy levels have been compared in Figure 4. The diagram depicts the model dependence of the (Ad) complex energy levels compared to the stability of the (Hb) energy levels. Also displayed is the increasing role of correlation in the determination of the *Q* quantities when the ZOH(2) clusters are used.

Finally, the ω(O−H) harmonic frequencies have been recalculated for each B(*n*)/ZOH(*i*) complex and compared to those of their isolated cluster analogues (Table 7). In all cases, bonding formation lowers the frequencies by about 200 cm^{-1}.

b. Chemical Shielding Tensors. The GIAO method has been applied at the HF/6-31G* level. For the (Hb) complex ZOH(2)/$(CH_3)_2CO$, results obtained with the extended basis sets 6-31+G* and 6-31++G** are also given. The maximum difference between the three sets of data is less than 5 ppm.

TABLE 6: Energies of Adsorption (Q_{ad}), Reaction (Q_{rea}), and Activation (Q_{ac}) Calculated Using 6-31G* Basis Set, Uncorrected (Q') and Corrected (Q) for Zero-Point Energy (ZPE) and Basis Set Superposition Error (BSSE) (Energies are in kJ/mol)

	HF				MP2//MP2			
systems	Q'_{ad}	ΔQ^{ZPE}	ΔQ^{BSSE}	Q_{ad}	Q'_{ad}	ΔQ^{ZPE}	ΔQ^{BSSE}	Q_{ad}
ZOH(1)	−52.1	8.3	8.7	−35.1	−60.7	8.7	18.2	−33.8
H_2CO ZOH(2)	−50.1	8.7	8.4	−33.0	−66.5	8.0	18.7	−39.0
ZOH(F)	−66.9	8.3	11.1	−47.5	−85.3	8.2	23.2	−53.9
ZOH(RS)	−48.2	9.7						
ZOH(RS,F)	−56.9	10.1						
ZOH(1)	−50.5	6.7	9.6	−34.2	−68.7	7.1	21.4	−40.2
(Hb) CH_3HCO ZOH(2)	−50.9	6.8	8.4	−35.7	−69.7	4.3[a]	11.5[a]	−53.9[a]
ZOH(F)	−67.1	6.1	10.9	−50.1	−87.5	4.5[a]	26.0[a]	−57.0[a]
ZOH(1)	−52.6	6.0	10.6	−36.0	−63.8	6.8	25.3	−31.7
$(CH_3)_2CO$ ZOH(2)	−46.6	3.3	7.0	−36.3	−61.0[a]	3.2[a]	12.9[a]	−44.9[a]
	(51.1)[b]		(6.0)[b]					
	(50.3)[c]		(4.6)[c]					
ZOH(F)	−73.1	5.2	12.2	−55.7	−95.0[a]	2.6[a]	23.2[a]	−69.2[a]
	Q'_{ac}	ΔQ^{ZPE}	Q_{ac}	Q'_{ac}	ΔQ^{ZPE}	Q_{ac}		
ZOH(1)	64.4	−1.7	62.7	28.4	0.9	29.3		
H_2CO ZOH(2)	79.4	−3.3	76.1	43.1	−4.2	38.9		
ZOH(1)	66.0	−6.6	59.4	38.0	−2.5	35.5		
(TS) CH_3HCO ZOH(2)	69.8	1.2	75.6					
$(CH_3)_2CO$ ZOH(1)	74.4	−4.2	70.2	39.0	−4.5	34.5		
	Q'_{rea}	ΔQ^{ZPE}	Q_{rea}	Q'_{rea}	ΔQ^{ZPE}	Q_{rea}		
ZOH(1)	−31.2	16.5	−14.7	−32.3	14.6	−17.7		
H_2CO ZOH(2)	−15.4	16.6	1.2	−25.7	14.9	−10.8		
ZOH(F)	8.6	14.5	23.1	−2.5	12.4	9.9		
ZOH(1)	−10.5	14.9	4.4	−21.1	13.3	−7.8		
(Ad) CH_3HCO ZOH(2)	13.5	15.7	29.2	−7.4	15.0a	7.6		
ZOH(F)								
ZOH(1)	3.6	13.3	16.6	−14.8	11.3	−3.5		
$(CH_3)_2CO$ ZOH(2)	48.8	12.7	61.5					
	(53.3)[b]							
	(53.2)[c]							

[a] Results obtained at MP2//HF/6-31G* level. [b] Calculated at HF/6-31+G*//6-31G* level. [c] Calculated at HF/6-31++G**//6-31G* level.

Thus, conclusions based on data provided by 6-31G*-type calculations are not significantly altered by the use of an improved basis set. The calculated components of the tensor are given in Table 8. It contains only the diagonal values of the tensor in the principal axis system. In this system, where with respect to the molecular frame, the *y* axis, as before, lies essentially along the CO bond, with the *z* axis perpendicular to the sp^2 plane. The values given in Table 8 are relative to the calculated trace of the tensor for TMS (tetramethylsilane) σ_{iso} (TMS) = 201.8 ppm. Only in the case of the hydrogen bonded complexes of acetone and acetaldehyde can a comparison be made with theory. For acetone, the three components along the principal axis have been measured from the powder line shape in the rigid lattice (ref 4). Relative to the isotropic shift of low-pressure gaseous TMS at room temperatures, these are σ_{11} = 318 ppm, σ_{22} = 280 ppm, σ_{33} = 83 ppm, and σ_{iso} = 227 ppm. For acetaldehyde, only the isotropic shift of the hydrogen bonded complex at room temperature σ_{iso} = 212 ppm, is available.[19]

V. Discussion

With present day ab initio calculations of the structure and electronic properties for relatively small molecules (10−20 electrons) it is possible to obtain results in excellent agreement with experiment. However, in this case, because of the size of systems it was necessary to reduce the size of the basis set and limit the electron correlation expansion to second order. The test of the accuracy of this approach is provided in Tables 1 and 2 where we have compared several calculated properties of the adsorbate molecules with experiment. In general, the agreement is reasonably good with both magnitude and trend on increasing the system size. In the case of the chemical shielding tensor (Table 2), however, fair agreement with experiment can only be obtained at the HF level. The correction for electron correlation to second-order MP2//HF in general underestimates the size of the anisotropy. This has been verified in the cases of CH_3CN[20] and H_2CO where the calculated HF anisotropies are 304.1 and 160.4 ppm, respectively, which compare favorably with experimental data at 318.0[20] and 158.4 ppm.[8] The same quantities, calculated with the MBPT(2)[21] program (correction for correlation effect) are lowered to 266.0 and 127.1 ppm.

The importance of considering the model cluster ZOH(F) is to explore the effect of relaxation. The optimization of this structure in the case of ZOH(1) and ZOH(2) gives rise to significant changes in structural parameters as shown in Table 3. The ZOH(F) structure, based on crystallographic parameters, is undoubtedly more characteristic of a true zeolite framework. In the calculations involving optimization on complex formation, the effects of relaxation are attenuated because constraints in the system increase, but the reduction is not significant. In all cases, the optimized results involving the ZOH(1) and ZOH(2) clusters overestimate the relaxation while ZOH(F), the other extreme, completely neglects it. Relaxation is clearly important since even these primitive simulations of the zeolite indicate that the silyl−ether addition complex cannot be stabilized unless it is allowed.

Unfortunately, in the case of both the hydrogen-bonded and addition complexes there is very little experimental data with

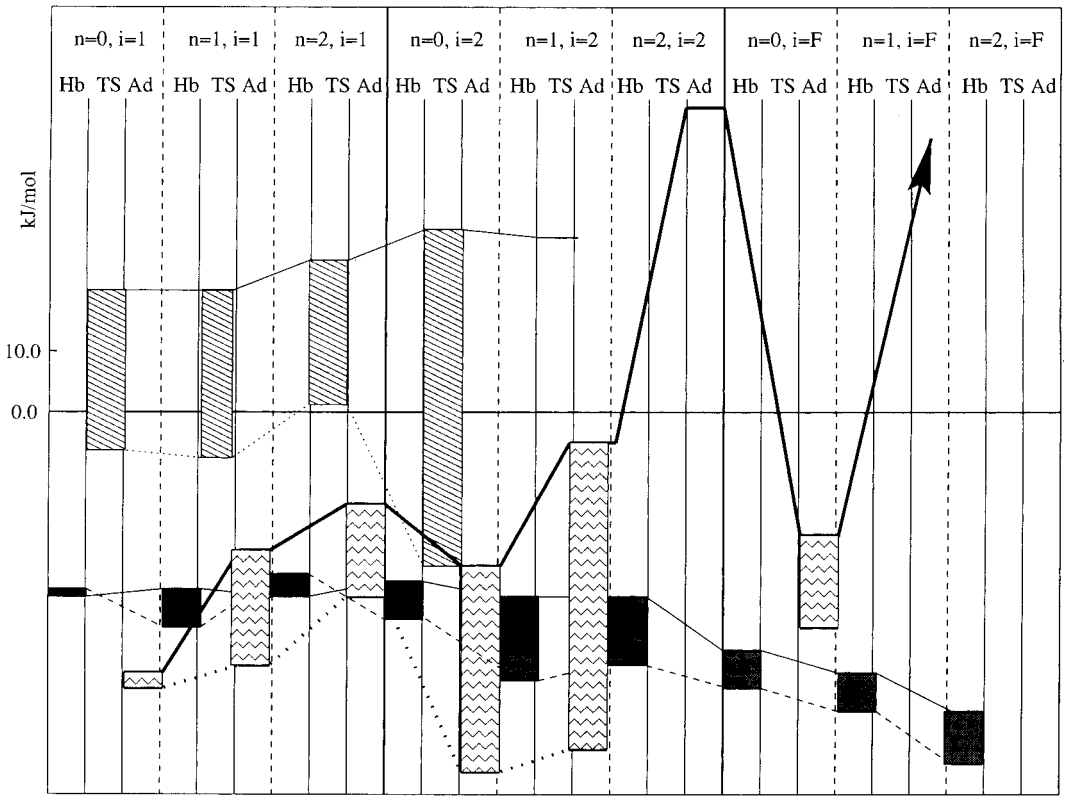

Figure 4. Diagram of energy levels of the complexes (Hb), (TS), and (Ad). Continuous and dotted lines connect energy levels calculated within (HF) and (MP2//MP2) approximations.

TABLE 7: Calculated Harmonic Frequencies ω_{OH}, at the HF (scaled) and MP2 Level Using the 6-31G* Basis Set of the Hydroxil Group at the Brönsted Site for Isolated Cluster ZOH(i) and (Hb) Complexes B/ZOH(i) (in cm^{-1})[a]

	HF		MP2//MP2	
systems	ω_{OH}	$\Delta\omega_{OH}$	ω_{OH}	$\Delta\omega_{OH}$
ZOH(1)	3574		3603	
ZOH(2)	3622		3692	
ZOH(F)	3491		3609	
ZOH(1)	3350	224	3338	265
H_2CO ZOH(2)	3336	286	3253	439
ZOH(F)	3387	104	2804	805
ZOH(1)	3362	212	3307	295
CH_3CHO ZOH(2)	3336	286		
ZOH(F)	3421	70		
ZOH(1)	3384	190	3278	325
$(CH_3)_2CO$ ZOH(2)	3457	165		
ZOH(F)	3251	240		

[a] $\Delta\omega_{OH} = \omega_{OH}$ (ZOH(i)) $- \omega_{OH}$ (B(n)/ZOH(i)).

TABLE 8: Calculated ^{13}C Chemical Shift Tensor Components of (Hb) and (Ad) Complexes B(*n*)/ZOH(*i*) at the HF/6-31G* Level[c]

systems	σ'_{xx}	σ'_{yy}	σ'_{zz}	σ^r_{iso}
H_2CO	274	191	72	179
CH_3CHO	281	199	73	200
$(CH_3)_2CO$	279	226	72	192
ZOH(1)	281	244	66	197
H_2CO ZOH(2)	276	238	67	194
ZOH(F)	277	248	66	197
ZOH(1)	291	241	68	200
(Hb) CH_3CHO ZOH(2)	293	230	71	198
ZOH(F)	299	235	72	200
ZOH(1)	283	278	69	210
$(CH_3)_2CO$ ZOH(2)	277	271	70	206
	282[a]	273[a]	70[a]	209[a]
	287[b]	273[b]	70.5[b]	209[b]
ZOH(F)	297	278	68	214
ZOH(1)	106	74	56	79
H_2CO ZOH(2)	105	82	56	81
ZOH(F)	125	114	54	98
ZOH(1)	101	84	64	86
(Ad) CH_3CHO ZOH(2)	113	95	62	90
ZOH(F)				
ZOH(1)	107	101	66	91
$(CH_3)_2CO$ ZOH(2)	116	106	69	97
ZOH(F)				

[a] Calculated at HF/6-31+G*//6-31G* level. [b] Calculated at HF/6-31++G**//6-31G* level. [c] Calculated values are referred to TMS. The chemical shift components of TMS, calculated at HF/6-31G* level are, respectively, $\sigma_{xx} = \sigma_{yy} = 200.1$ ppm, $\sigma_{zz} = 204.9$ ppm and $\sigma_{iso} = (1/3)(\sigma_{xx} + \sigma_{yy} + \sigma_{zz})$ ppm. The data given in the table are: $\sigma^r_{\alpha\alpha}$ ($\alpha = x$, y, z, or iso) $= \sigma_{iso}$(TMS) $- \sigma_{\alpha\alpha}$ (calculated).

which to make a comparison. Parrillo et al.[22] have shown in the case of strong bases such ammonia and amines that there is a linear correlation between the differential heat of adsorption and the gas-phase proton affinity of the base. Only in the case of the ZOH(F) complex does one find that trend (see Table 6 and Figure 5). Similarly, if one compares the calculated heat of adsorption, Q_{ad} of acetone with experiment, the only case where data is available, then one finds again that the best agreement occurs with the larger cluster ZOH(F) complexed molecule. The calculated Q_{ad} when corrected for basis set superposition error and zero-point effects gives values of -55.7 and -67.0 kJ/mol at the HF and MP2//MP2 levels. This is to be best compared with the difference in differential heats of adsorption in HZSM-5 and silicalite[4] of 67.0 ∓ 3 kJ/mol. Since the silicalite contains no acid sites and the molecule−silicalite interactions are mainly electrostatic and van der Waals, then this difference corresponds closely to the heat required to form the hydrogen bond in the vicinity of the acid site. This relates more closely to the situation in the calculations where the

TABLE 9: Experimental and Theoretical Results within the ZOH(F) Cluster Model for (Hb) Complex Formed with Acetone (ref 4), Compared to Similar Theoretical Predictions for Formaldehyde and Acetaldehyde[b]

	$(CH_3)_2CO$						
	theory isolated molecule	theory H-Bond cluster	solid at 78 K	silicate at 78 K	HZSM-5 at 80 K	H_2CO theory H-Bond cluster	CH_3HCO theory H-Bond cluster
σ_{11}	279	296.6	283	298.0	318	277.4	299.1
σ_{22}	226	277.6	272	269	280	284.1	235.2
σ_{33}	72	68.5	84	88	83	65.6	71.9
σ_{iso}	192	214.2	213	219	227	197	200.1
σ_{aniso}	−180.5	−218.6	−193.5	−195.5	−216	−197.2	−195.7
q(C)	0.524*	0.578				0.155	0.372

[a] Does not fit properly the σ_{iso}/q(C) correlation, but theoretical estimation of σ_{iso}, for isolated species, are systematically underestimated with respect to experimental data (see Table 2). [b] Shifts are relative to theoretically calculated isolated TMS molecule. Experimental shifts (acetone) are relative to low-pressure gas TMS. q(C) is the calculated net atomic charge on the ^{13}C atom. Chemical shifts are in ppm and atomic charges in au. $\sigma_{aniso} = \sigma_{33} - 0.5(\sigma_{11} + \sigma_{22})$.

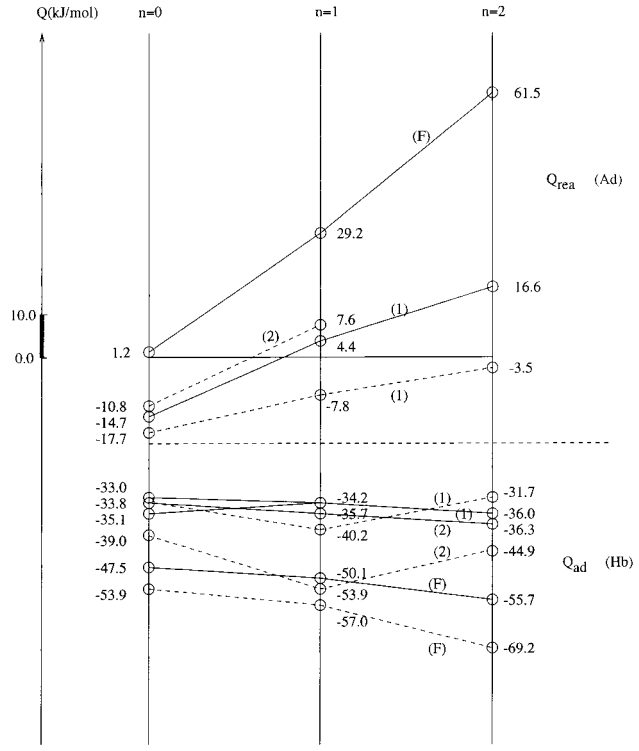

Figure 5. Variations of heat of adsorption (Q_{ad}) and heat of reaction (Q_{rea}) for the different adsorbats $H_{2-n}(CH_3)_nCO$ ($n = 0, 1, 2$). For each n, values corresponding to the three possible clusters ($i = 1$, 2, and F) are given at the HF level (continuous line) and MP2//MP2 level (dotted line). All values are in kJ/mol.

simulation of the zeolite confinement and embedding effects have in large part been ignored.

An examination of Table 9 also points to ZOH(F) as the model which gives better agreement between theory and experiment. The theory predicts that when the adsorbate acetone is complexed to form the hydrogen bonded species in the zeolite, the largest change occurs in σ_{yy}, the component along the C═O bond. Experimentally, this would correspond to σ_{22}. One finds experimentally that for carbonyl ^{13}C atoms this component is most susceptible to its environment[10] which appears to be the case in acetone when hydrogen bonding occurs. This environmental effect is also illustrated in Table 9 for acetone, where the larger changes in σ_{22} when a hydrogen bond is formed also occur when the molecule is confined in both the solid and the silicalite framework. However, it is important to remark that here "environmental" means here a local effect due to the formation of the hydrogen bond. Consequently, since HF calculations reproduce very well these hydrogen-bonding effects, an excellent agreement between the calculated and observed value of the σ_{yy} component (277.6 ppm versus 280.0 ppm) is obtained. Finally, the net charge on the ^{13}C atom is also given in Table 9. As already stated[23] in others cases, the decrease of electronic charge on the carbon atom corresponds to an increase of σ_{iso}.

Even though the above discussion strongly suggests that a very rigid zeolite framework gives better agreement between theory and experiment for certain properties, physically some relaxation must occur on complexing with an adsorbed species. Since structural relaxation tends to stabilize a silyl−ether addition compound, one cannot completely exclude the importance of this complex in chemical changes. The calculations do however indicate that the larger the cluster size the less stable the addition compound, suggesting that more and more of the "nonlocal" interactions are taken into account. This effect would limit framework relaxation. Hence, the smaller the adsorbate molecule, the greater the likelihood of forming the addition compound. Finally, test calculations with larger basis set functions or larger clusters show that our results are not qualitatively affected by these effects.

Acknowledgment. The authors thank the "Institut du Développement des Ressources en Informatique Scientifique" (IDRIS) from CNRS for the attribution of computing ressources (Project 980345). D.W. acknowledges partial support from an NSF Grant CTS9713023 and M.A. for support from the "French Institute for Culture and Technology", University of Pennsylvania. The authors thank also Dr. P. Pulay for providing his program and Drs. R. J. Gorte and E. M. Evleth for helpful discussions.

References and Notes

(1) (a) Kotrla, J.; Nachtigallovà, D.; Kubelkovà, L.; Heeribout, L.; Doremieux-Morin, C.; Fraissard, J. *J. Phys. Chem. B* **1998**, *102*, 2454. (b) Limtrakul, J. *Chem. Phys.* **1995**, 193, 79.

(2) (a) Evleth, E. M.; Kassab, E.; Jessri, H.; Allavena, M.; Montero, L.; Sierra, L. R. *J. Phys. Chem.* **1996**, *100*, 11368. (b) Sierra, L. R.; Kassab, E.; Evleth, E. M. *J. Phys. Chem.* **1993**, *97*, 641.

(3) Gorte, R. J.; White, D. *Top. Catal.* **1997**, *4*, 57.

(4) Sepa, J.; Lee, C.; Gorte, R. J.; White, D.; Kassab, E.; Evleth, E. M.; Jessri, H.; Allavena, M. *J. Phys. Chem.* **1996**, *100*, 18515.

(5) (a) Vetrivel, R.; Catlow, C. R. A.; Colbourn, E. A. *Proc. R. Soc. London A* **1988**, *417*, 81. (b) Allavena, M.; Seiti, K.; Kassab, E.; Ferenczy, Gy.; Angyan, J. G. *Chem. Phys. Lett.* **1990**, *168*, 461. (c) Aloisi, G.; Barnes, P.; Catlow, C. R. A.; Jackson, R. A.; Richards, A. J. *J. Phys. Chem.* **1990**, *93*, 3573. (d) White, J. C.; Hess, A. C. *J. Phys. Chem.* **1993**, *97*, 8703. (e) Teunissen, E. H.; Jansen, A. P. J.; van Santen, R. A.; Orlando, R.; Dovesi, R. *J. Chem. Phys.* **1994**, *101*, 5865. (f) Kyrlidis, A.; Cook, S. J.; Chakraborty, A. K.; Bell, A. T.; Theodorou, D. N. *Phys. Chem.* **1995**, *99*, 1505. (g) Teunissen, E. H.; Jansen, A. P. J.; van Santen, R. A. *J. Phys. Chem.* **1995**, *99*, 1873. (h) Eichler, U.; Brändle, M.; Sauer, J. *J. Phys. Chem. B.* **1997**, *101*, 10035. (i) Brändle, M.; Sauer, J. *J. Am. Chem. Soc.* **1998**, *120*, 1556.

(6) Frisch, M. J.; Trucks, G. W.; Schlegel, H. B.; Gill, P. M. W.; Johnson, B. G.; Robb, M. A.; Cheeseman, J. R.; Keith, T. A.; Petersson, G. A.; Montgomery, J. A.; Raghavachari, K.; Al-Laham, M. A.; Zakrzewski, V. G.; Ortiz, J. V.; Foresman, J. B.; Cioslowski, J.; Stefanov, B. B.; Nanayakkara, A.; Challacombe, M.; Peng, C. Y.; Ayala, P. Y.; Chen, W.; Wong, M. W.; Andres, J. L.; Replogle, E. S.; Gomperts, R.; Martin, R. L.; Fox, D. J.; Binkley, J. S.; Defrees, D. J.; Baker, J.; Stewart, J. P.; Head-Gordon, M.; C. Gonzalez, C.; Pople, J. A. *Gaussian 94*, revision C.3; Gaussian, Inc.: Pittsburgh, PA, 1995.

(7) Wolinski, K.; Hinton, J. F.; Pulay, P. *J. Am. Chem. Soc.* **1990**, *112*, 8251.

(8) Pulay, P. *TEXAS-90*; Department of Chemistry and Biochemistry, The University of Arkansas: Fayetteville, AR. Copyright (Program and description) Pulay, P. and co-workers.

(9) Wu, G.; Lumsden, M. D.; Ossenkamp, G. C.; Eichele, K.; Wasylishen, R. E. *J. Phys. Chem.* **1995**, *99*, 15806.

(10) Zilm, K. W.; Grant, D. M. *J. Am. Chem. Soc.* **1981**, *103*, 2913.

(11) Spiess, H. W. In *NMR Basic Principles*; Springer: New York, 1978; Vol. 15, p 55.

(12) Mortier, W.; van den Bossche, E.; Uytterhoeven, J. B. *Zeolites* **1984**, *4*, 41.

(13) Smith, J. V. *Chem. Rev.* **1988**, *88*, 149.

(14) Czjzek, M.; Jobic, H.; Fitch, A. N.; Vogt, T. *J. Phys. Chem.* **1992**, *96*, 1535.

(15) Makarova, M. A.; Ojo, A. F.; Karim, K.; Hunger, M.; Dwyer, J. *J. Phys. Chem.* **1994**, *98*, 3619.

(16) Mirsojew, I.; Ernst, S.; Weitkamp, J.; Knözinger, H. *Catal. Lett.* **1994**, *24*, 235.

(17) Jacobs, W. P. J. H.; van Wolput, J. H. M. C.; van Santen, R. A. *Zeolites* **1994**, *14*, 117.

(18) Jacobs, W. P. J. H.; Jobic, H.; van Wolput, J. H. M. C.; van Santen, R. A. *Zeolites* **1992**, *12*, 315.

(19) Biaglow, A. I.; Sepa, J.; Gorte, R. J.; White, D. *J. Catal.* **1995**, *151*, 373.

(20) Sepa, J.; Gorte, R. J.; White, D.; Kassab, E.; Allavena, M. *Chem. Phys. Lett.* **1996**, *262*, 321.

(21) Bartlett, R. J. *Quantum Theory Project 362*; Williamson Hall, University of Florida: Gainsville, FL.

(22) Parrillo, D. J.; Gorte, R. J.; Farneth, W. E. *J. Am. Chem. Soc.* **1993**, *115*, 12441.

(23) (a) Fliszar, S.; Cardinal, G.; Béraldin, M.-T. *J. Am. Chem. Soc.* **1982**, *104*, 5287. (b) Ortiz, P. J.; Evleth, E. M.; Montero, L. A. *J. Mol. Struct. (THEOCHEM)* **1998**, *432*, 121.